

VOLTAGE-ACTIVATED CURRENTS IN SOMATIC MUSCLE OF THE NEMATODE PARASITE *ASCARIS SUUM*

BY R. J. MARTIN, P. THORN, K. A. F. GRATION AND I. D. HARROW

Department of Preclinical Veterinary Sciences, R. (D.) S.V.S., Summerhall, University of Edinburgh, Edinburgh, EH9 1QH and Animal Health Discovery, Pfizer Central Research, Sandwich, Kent, CT13 9NJ

Accepted 3 August 1992

Summary

1. Voltage-activated currents in cell bodies of the somatic muscle cells of *Ascaris suum* were studied using a two-microelectrode voltage-clamp technique. Cells recorded from had resting membrane potentials around -35 mV and had input conductances in the range 1 – 10 μ S.

2. In cells bathed in artificial perienteric fluid, depolarizing steps from a holding potential of -35 mV elicited outward currents at a threshold of -15 mV. These currents had inwardly directed inflections on the rising phase, suggesting the presence of more than one current. Hyperpolarizing steps did not activate current.

3. Tetraethylammonium (TEA^+ , 69 mmol l^{-1}) blocked the outward currents and allowed a voltage-dependent inactivating Ca^{2+} current to be observed. The peak current–voltage relationship was U-shaped with a threshold around -15 mV and peak at $+5$ mV. The reversal potential of the Ca^{2+} current was estimated by extrapolation to be $+45$ mV.

4. The permeability of the voltage-activated outward currents was studied by examining reversal potentials of tail currents. The reversal potentials were linearly dependent on the logarithm of the extracellular potassium concentration if extracellular $[\text{K}^+]$ was greater than 10 mmol l^{-1} . The Na^+/K^+ permeability ratio of the currents was 0.04 .

5. Inactivation, seen as a decline following the peak of the K^+ current, was produced by maintained depolarization. The recovery from inactivation was complex and could be described by the sum of two exponentials with time constants of 0.67 s and 20.1 s. Steady-state inactivation of the K^+ currents was observed at a range of holding potentials. Only a proportion (34%) of the total K^+ current was inactivated by holding potentials more positive than -20 mV.

6. Extracellular application of 5 mmol l^{-1} 4-aminopyridine (4-AP) selectively abolished an early fast component of the K^+ current (the peak). The 4-AP-sensitive current decayed quickly with a time constant of around 10 ms; a Boltzmann fit to its activation curve had a half-maximal activation voltage of $+14$ mV and a 'slope' of 10.5 mV. The 4-AP-resistant current decayed with a time constant of around 1 s; a Boltzmann fit to its activation curve had a half-maximal activation voltage of $+29$ mV and a 'slope' of 12 mV.

Key words: *Ascaris suum*, voltage-clamp, muscle, calcium currents, potassium currents.

7. Depolarization activates a Ca^{2+} current and two K^{+} currents: the K^{+} currents were separated into lower-threshold, fast-inactivating (I_a -like) and higher-threshold, slowly inactivating (I_k -like) currents.

Introduction

Ascaris suum is an intestinal nematode parasite of pigs and is capable of maintaining its position in the gut by means of forwardly directed waves of contraction. The somatic muscle cell of *Ascaris* consist of a contractile spindle region; a balloon-shaped structure, the bag which contains the nucleus; and a thin process known as the arm which passes to a nerve cord where it is electrically coupled to adjacent cells and where it receives excitatory and inhibitory synaptic inputs (Rosenbluth, 1963, 1965). DeBell *et al.* (1963) and Weisblat *et al.* (1976) have studied the electrophysiology of *Ascaris* body muscle cells and described three types of depolarizing potential recorded in the bag region of the muscle which are related to contraction. They described the 'spike potentials', the 'slow waves' and the 'modulation waves'. The spike potentials were of varying amplitude up to 30 mV, lasted 5–10 ms and behaved like Ca^{2+} spikes; the slow waves were up to 20 mV in amplitude and lasted 100–1000 ms; the modulation waves lasted several seconds, were up to 5 mV in amplitude but were directly associated with muscle contraction. The currents responsible for depolarization and repolarization of the cells have yet to be isolated and identified.

Muscle cells of *Ascaris* are large enough to allow a two-microelectrode voltage-clamp to be used to examine membrane currents (Martin, 1982). This technique has revealed the presence of a voltage-sensitive Ca^{2+} current and two K^{+} currents that underlie the spike potential and are the subject of this paper.

Materials and methods

The preparation

Ascaris suum, approximately 20 cm in length, were obtained from the local slaughterhouse, maintained in Locke's solution at 32 °C and used within 4 days. An anterior section of the worm, 2 cm long, was cut along a lateral line and then pinned cuticle side down onto a layer of Sylgard in the experimental chamber. The gut was then removed, exposing the muscle cell bodies. The experimental chamber consisted of a central bath with a liquid capacity of 1.8 ml. The bath was surrounded by a water jacket through which water was circulated to maintain the preparation at 37 °C. The worm was viewed from above through a Bausch and Lomb zoom microscope and cross illuminated using a fibre-optic light source. The preparation was continuously perfused with a Shuco pump and, by means of a broken pipette, positioned near (500 μm) the cell recorded from, in order to accelerate solution changes. The flow rate for the total perfusion system was set at 8 ml min^{-1} and cleared the bath in 4.5 min when filled with blue dye. An interval of 7–15 min was therefore used after a change of solution and before recording.

Electrodes

Two micropipettes were placed in the bag region of the muscle cells in order to carry

out the two-microelectrode voltage-clamp experiments. The micropipettes were pulled on a David Kopf puller from filamented glass tubing (Clarke Electromedical Instruments GC 150F-15). The current micropipettes had a resistance of $4\text{ M}\Omega$ and the voltage micropipette had a resistance of $11\text{ M}\Omega$. Both were filled with 3 mol l^{-1} potassium acetate. 3 mol l^{-1} magnesium sulphate was used to fill the micropipettes when reversal potentials were being measured.

Solutions

Initially artificial perienteric fluid (APF) was used which contained (mmol l^{-1}): NaCl, 23; sodium acetate, 110; KCl, 24; CaCl_2 , 6; MgCl_2 , 5; glucose, 11; Hepes, 5; pH 7.6 with NaOH. For recording Ca^{2+} currents, a solution with TEA⁺ to block K⁺ currents and a high Ca^{2+} concentration was used containing (mmol l^{-1}): TEACl, 69; calcium acetate, 69; potassium acetate, 24; magnesium acetate, 5; glucose, 11; pH 7.6 with maleic acid. In most of the experiments described here, a Ca^{2+} -free lanthanum solution based on *Ascaris* Ringer was used which contained (mmol l^{-1}): NaCl, 135; KCl, 3; MgCl_2 , 15.7; glucose, 3; Tris, 5; EGTA, 0.5; LaCl, 1; pH 7.6 with maleic acid. The use of this type of low- Ca^{2+} solution is likely to abolish secondary channel currents produced as a result of entry of Ca^{2+} into the cell: one example of this type of channel current in *Ascaris* is the Ca^{2+} -activated Cl^- channel (Thorn and Martin, 1987). In order to modify the reversal potential of tail currents, Ca^{2+} -free lanthanum solutions were used in which sodium was substituted for potassium; they contained (mmol l^{-1}): NaCl, 0.1–138; KCl, 0.1–138 (total $\text{K}^+\text{+Na}^+=138$); MgCl_2 , 15.7; glucose, 3; Tris, 5; EGTA, 0.5; LaCl, 1; pH 7.6 with maleic acid.

Recording system

A Dagan 8500 voltage-clamp was used and all output was displayed on a Gould OS400 digital storage oscilloscope with an IEEE 488 interface. The gain on the amplifier was adjusted to 2500–5000 V/V and the phase lag was adjusted for each cell to give optimal recording. Data were recorded on a Racal Store Four DS tape recorder with a bandwidth of up to 2.5 kHz. The signal was played back into a Lectromed chart recorder or a Gould Series 6000 XY plotter to provide hard copy. All pulse regimes were controlled by a Digitimer D100. Stimulus input was provided by Digitimer DS2 isolated stimulators. Leak subtraction, where used, was performed by summation of two current responses to equal but opposite-polarity voltage steps. The current response to hyperpolarizing steps was linear in the range used and therefore represented the leak current.

It was possible to check the quality of the space-clamp in the bag region of the muscle cell by placing a third micropipette in the base of the bag, at a site near the junction with the spindle, while the other two micropipettes for the voltage-clamp were placed at the top of the bag. Under these conditions it was found that the third micropipette could record a voltage response that was 95% of the command potential within $500\ \mu\text{s}$. In view of the particular anatomy of the muscle cells of *Ascaris* it is, however, likely that there may be poorly controlled regions of membrane: these were recognised as 'notches' of inward current which occurred at a relatively long but irregular time after the start of the depolarizing pulse, producing a very abrupt rise in the inward current-voltage

relationship. Such events led to the rejection of the muscle cell for recording: only currents from cells which showed adequate voltage control were analysed.

Data analysis

The peak amplitude and time to peak of current responses were measured from graphs of currents plotted against time. The limiting equivalent voltage sensitivity for the Ca^{2+} current was determined from the maximum slope of the plot of $\log_e(\text{peak } \text{Ca}^{2+} \text{ current}/\text{maximum peak } \text{Ca}^{2+} \text{ current})$ against voltage (Hille, 1984). A BBC microcomputer with a Unilab interface was used to digitize the currents. Sampling rates were adjusted between 1 kHz and 0.05 kHz, depending on the duration the sample. The rate of decay was then analysed using the BMDP P3R non-linear regression program. The best fits to the Boltzmann equation were obtained using the NAG subroutine E04CCF.

Results

This paper describes results from 49 successful voltage-clamp experiments. The resting membrane potentials of recorded muscle cells were around -35 mV with a mean input conductance of $2.4 \pm 0.18 \mu\text{S}$ (mean \pm S.E., $N=9$) measured using 150 ms hyperpolarizing voltage pulses.

Depolarizing voltage steps from a holding potential of -35 mV elicited an outward current in cells bathed in APF solution (Fig. 1A). These currents rose to a peak within 20 ms and had an inwardly directed inflection in the rising phase: these inflections were not because of 'breakthrough' as a result of poor space-clamping because they occurred in most cells at regular intervals after the onset of the depolarizing pulse. After the peak current there was a slow decay. As the depolarizing steps were made more positive, the outward-current peak became more pronounced. Hyperpolarizing steps did not induce active currents (Fig. 1B). A plot of current amplitude 20 ms after the voltage step against the potential shows the current increasing non-linearly on depolarization but linearly on hyperpolarization (Fig. 1C). The linearity observed following hyperpolarization was subsequently used to allow for 'leakage' correction.

Inward currents

In five experiments, substitution of sodium in APF with 69 mmol l^{-1} tetraethylammonium (TEA^+) and 69 mmol l^{-1} calcium revealed an inward current activated by depolarizing voltage-clamp steps from a holding potential of -35 mV. This inward current was identified as a Ca^{2+} current on the grounds that the permeant cation was calcium in the high- Ca^{2+} TEA^+ solution. As further confirmation of the identity of the inward current, it was found that bath-application of lanthanum (using 1 mmol l^{-1} LaCl) as a calcium channel blocker rapidly abolished the inward current (not shown). The Na^+ channel blocker tetrodotoxin was not used because of its lack of effect in *Ascaris* (Jarman and Ellory, 1969). A family of Ca^{2+} currents evoked by increasing depolarizing steps and corrected for leakage is shown in Fig. 2A. The threshold for activation of the inward current was around -15 mV. More depolarized voltage-clamp steps increased the amplitude of the inward-current peak up to a value of about $+5$ mV and thereafter

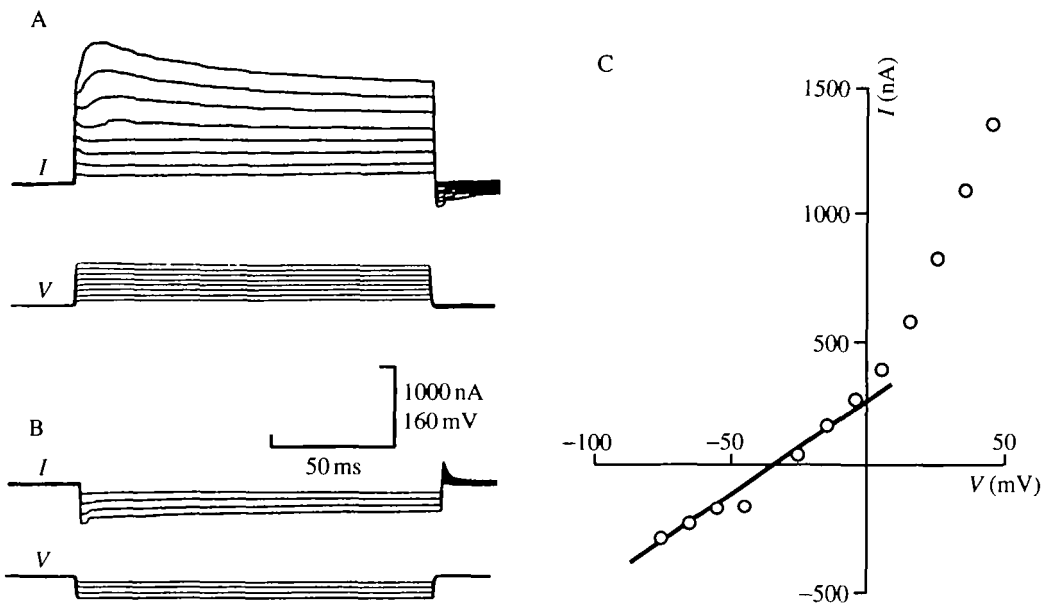


Fig. 1. Family of currents obtained from a cell under voltage-clamp bathed in APF. The current records are labelled *I* and voltage records are labelled *V*. The cell was stepped from a holding potential of -35 mV, in increments of 10 mV, to a series of step potentials (Sp). (A) Sp= -25 mV, -15 mV, -5 mV, 5 mV, 15 mV, 25 mV, 35 mV, 45 mV. (B) Sp= -45 mV, -55 mV, -65 mV, -75 mV, -85 mV, -95 mV, -105 mV. (C) Current-voltage plot from the same experiment as that of A and B. The peak current was measured 20 ms after the start of the step potential. The straight line illustrates the linear portion of the plot suitable for leakage correction.

decreased it with further depolarization; the time to peak decreased monotonically with increasing depolarization. At the most depolarized potentials, the peak of the inward current was followed by a small outward current which may be because of residual outward current not blocked by TEA^+ . However, there was no evidence of any maintained current; at the end of the 150 ms pulses all the currents had inactivated and there was tail current on the return to the holding potential of -35 mV. The time constant for inactivation of the Ca^{2+} current was, therefore, less than 150 ms, the length of the voltage pulse. All the data from this cell relating peak inward current to voltage are shown in Fig. 2B. The maximum inward current was 411 nA, the extrapolated reversal potential was $+45$ mV and the limiting equivalent voltage-sensitivity (Hille, 1984) was 7.5 mV per e-fold increase in Ca^{2+} current.

The predicted Nernst Ca^{2+} potential with 69 mmol l^{-1} extracellular calcium and 1 $\mu\text{mol l}^{-1}$ intracellular calcium is $+140$ mV, some 95 mV more positive than estimated here. Despite the theoretical prediction of $+140$ mV, many other authors report values as low as $+40$ mV to $+70$ mV, which they explain by the Ca^{2+} channels also being permeable to other monovalent ions (K^+) moving outwards through the Ca^{2+} channels (Reuter and Scholtz, 1977; Fenwick *et al.* 1982; Lee and Tsien, 1982).

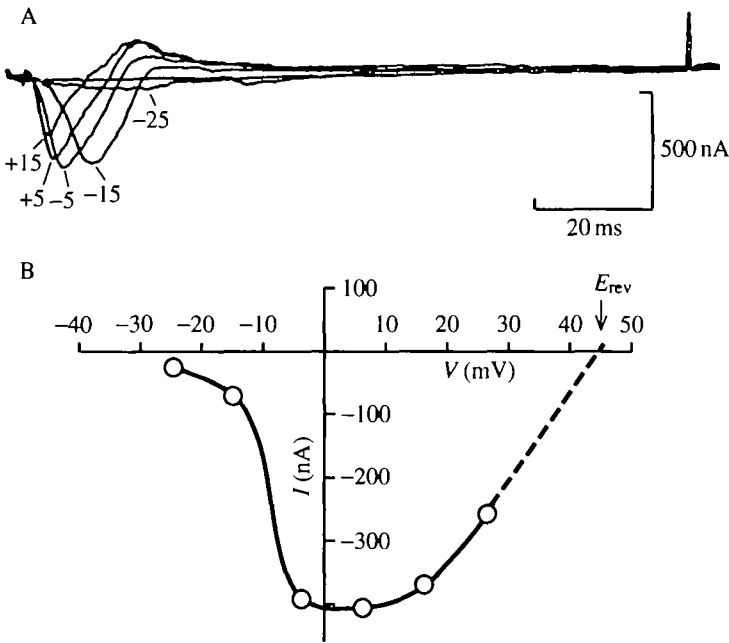


Fig. 2. (A) Leak-subtracted current-voltage relationship in a cell bathed in TEA⁺ APF and 69 mmol l⁻¹ Ca²⁺. The cell was stepped from a holding potential of 35 mV to -25 mV, -15 mV, -5 mV, +5 mV, +15 mV and +25 mV; paired hyperpolarizing pulses were used for the leak subtraction procedure. Increased depolarizing steps increased and then decreased the inward current and decreased the time to peak current. A small outward current is also seen following the inward current. A capacitive current is seen at the end of the pulse but is not so apparent at the beginning because of the leak subtraction process used. (B) Peak Ca²⁺ current-voltage plot. Extrapolation of the plot gives an estimate of +45 mV for the reversal potential at 37 °C.

Effect of changing extracellular potassium concentration on the reversal potential of the tail current

The aim of this series of experiments was to examine the permeability of the outward current activated by depolarization. The experimental approach was to activate the currents and then to determine the reversal potentials of the tail currents at different potentials, in solutions of different potassium concentrations (Fig. 3A-D). Cells were bathed in Ca²⁺-free lanthanum solutions to block Ca²⁺ currents (Meech and Standen, 1975; Thomas, 1984) and potassium was replaced by sodium. The experiments were carried out using a two-pulse voltage-clamp protocol: i.e. a holding potential of -35 mV, a prepulse potential of +55 mV for 10-20 ms to activate the outward current and a step potential to between -125 mV and +55 mV. The amplitude and duration of the tail current elicited during the step potential then allowed the reversal potentials of the current activated by depolarization to be determined.

Fig. 3A shows representative currents obtained from a cell bathed in 0.1 mmol l⁻¹ potassium. Fig. 3B,C,D shows the currents obtained in 3 mmol l⁻¹, 30 mmol l⁻¹ and

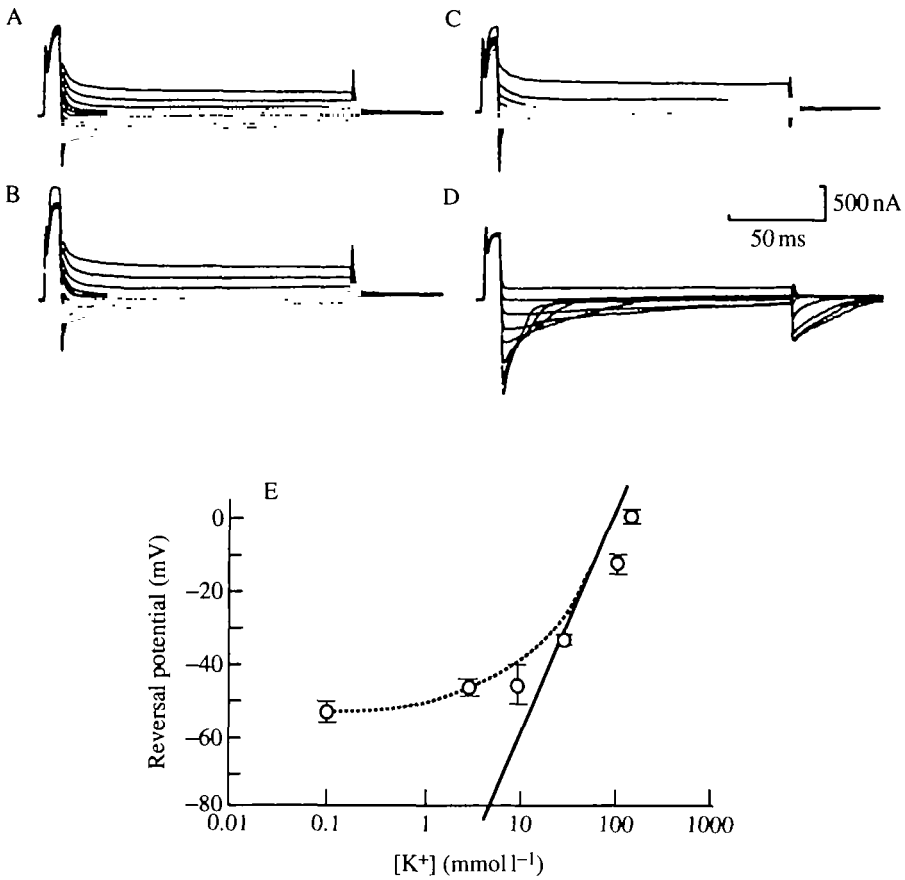


Fig. 3. Estimation of tail current reversal potentials in solutions of different K⁺ concentration. A two-step protocol was used: the holding potential was -35 mV; the first step was to +55 mV for 10 ms to activate the current; the potential of the second voltage step was varied to determine the reversal potential of the tail current. In A, B and C the second steps were to -125 mV, -115 mV, -105 mV, -95 mV, -85 mV, -75 mV, -65 mV, -55 mV, -45 mV, -25 mV, -15 mV, -5 mV, 0 mV, +5 mV, +15 mV. In D the second steps were to -95 mV, -85 mV, -75 mV, -65 mV, -55 mV, -45 mV, -25 mV, -15 mV. (A) 0.1 mmol l⁻¹ potassium lanthanum solution; (B) 3 mmol l⁻¹ potassium lanthanum solution; (C) 30 mmol l⁻¹ potassium lanthanum solution; (D) 138 mmol l⁻¹ potassium lanthanum solution. The cell was bathed for 10 min in each solution before recording the currents at 37 °C. (E) The mean \pm s.e. reversal potential, obtained from six experiments conducted in the same manner as the experiment illustrated in A, B, C and D is plotted as a function of log potassium concentration of the bathing solution. Reversal potentials were estimated from plots of tail-current amplitude against membrane potential. The points show linearity between 10 mmol l⁻¹ and 138 mmol l⁻¹ extracellular potassium, but at lower potassium concentrations the relationship was non-linear. The solid line on the graph was drawn according to the Nernst equation assuming an intracellular potassium concentration of 99.4 mmol l⁻¹ (Brading and Caldwell, 1971). The dotted line was drawn using the constant-field equation with a Na⁺/K⁺ permeability ratio of 0.04.

138 mmol l⁻¹ extracellular potassium, respectively. The reversal potential of the tail current moved in the depolarizing direction as extracellular potassium concentration increased. The means \pm s.e. of reversal potentials were then plotted against log potassium concentration (Fig. 3E). The plot was essentially linear for extracellular potassium concentrations above 10 mmol l⁻¹ but deviated below this concentration. The constant-field equation (Hille, 1984) for a channel current permeable to potassium and sodium predicts that:

$$E_{\text{rev}} = RT/F \log_e \left(\frac{\beta[\text{Na}^+]_o [\text{K}^+]_o}{\beta[\text{Na}^+]_i + [\text{K}^+]_i} \right), \quad (1)$$

where E_{rev} is the reversal potential, R , T and F have their usual meaning, $[\text{Na}^+]_o$ and $[\text{Na}^+]_i$ are the extracellular and intracellular sodium concentrations, $[\text{K}^+]_o$ and $[\text{K}^+]_i$ are the extracellular and intracellular potassium concentrations and β is the Na⁺/K⁺ permeability ratio. If the intracellular K⁺ concentration is taken as 99.4 mmol l⁻¹ (Brading and Caldwell, 1971) and β is set to zero then the reversal potential will be described by the Nernst equation shown by the solid line on the plot (Fig. 3E). If the intracellular sodium concentration is taken as 44.6 mmol l⁻¹ (Brading and Caldwell, 1971) and β set to 0.04 then the constant-field equation predicts the relationship shown by the broken line on the plot (Fig. 3E).

These experiments are consistent with depolarization activating cation channel currents which are about twenty times more permeable to potassium than to sodium. The extracellular potassium concentration is around 20 mmol l⁻¹ in *Ascaris* (Brading and Caldwell, 1971) and the reversal potential of the outward current is expected to be in the linear region of the plot (Fig. 3E) under physiological conditions. Subsequently in this paper the voltage-activated outward current is referred to as the K⁺ current.

Recovery of K⁺ current from inactivation

Prolonged depolarizing voltage steps produced a K⁺ current which rapidly rose to a peak and then slowly declined. This decline was taken to indicate slow inactivation of the K⁺ current during depolarization; at hyperpolarized potentials the inactivation would have to be removed to allow subsequent activation by depolarizing steps. In order to study the time course of recovery from inactivation, a two-step depolarizing protocol was used: the depolarizing steps were separated by intervals lasting up to 12 s at a holding potential of -35 mV (Fig. 4A). A delay of 1 min between each series of two depolarizing pulses was adequate to allow complete recovery of the K⁺ current.

It can be seen from Fig. 4A that there is selective inactivation of an early component of the K⁺ current (the peak), with the peak current amplitude of the second pulse recovering as the interpulse interval is lengthened. The time course of recovery from inactivation is shown in Fig. 4B, where the difference between the peak current and the steady-state current at the end of the second pulse was expressed as a percentage of the difference of first pulse: the value obtained represents the percentage recovery. The means \pm s.e. of the recovery percentages obtained from six experiments were then plotted as a function of the interpulse interval (Fig. 4B). The points were then fitted by the equation:

$$R = 100 \times \{A[1 - \exp(-t/T_1)] + B[1 - \exp(-t/T_2)]\}, \quad (2)$$

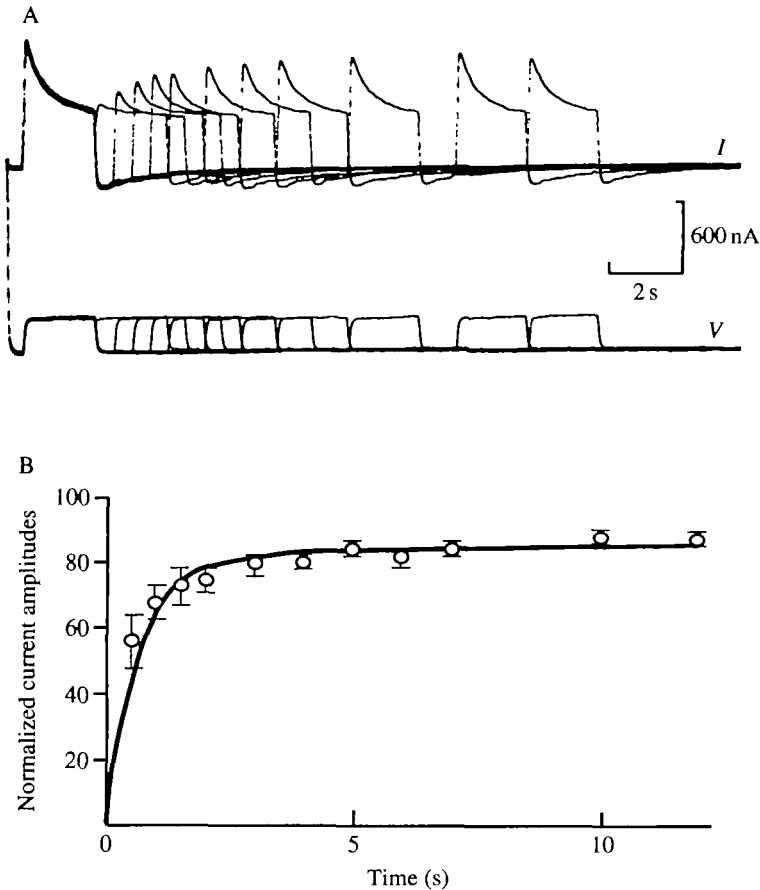


Fig. 4. Double-voltage-pulse estimation of the inactivation recovery time course. The cell was first stepped from a holding potential of -35 mV to a conditioning pulse of $+55$ mV; this was followed by a test pulse of $+55$ mV after increasing time intervals. The interpulse interval was measured as the time between the end of the conditioning pulse and the beginning of the test pulse. The interval was varied between 0 and 12 s. Ca^{2+} -free lanthanum solution. (A) Current (top) and voltage (bottom). The peak amplitude of the outward current activated by the test pulse was reduced at short interpulse intervals but showed a gradual recovery as the interpulse interval increased. (B) Plot of the difference between the peak current and steady-state current at the end of the test pulse expressed as a percentage of the same from the conditioning pulse. The means \pm s.e. of the recovery percentages obtained from six experiments are plotted as a function of the interpulse interval. The points were fitted to the recovery equation (equation 2). $A=0.825$, $T_1=0.67$ s, $B=0.087$ and $T_2=20.12$, 37°C .

where R is the percentage recovery, t is time, A and B are constants and T_1 and T_2 are the fast and slow time constants of recovery. T_1 was 0.67 s; T_2 was 20.1 s; A was 0.825 and B was 0.087 (line on Fig. 4B). Since A was large compared to B it follows that most of the recovery occurs in less than 2 s but full recovery was not observed after 12 s, the maximum test interval shown in Fig. 4B, since T_2 was 20.1 s.

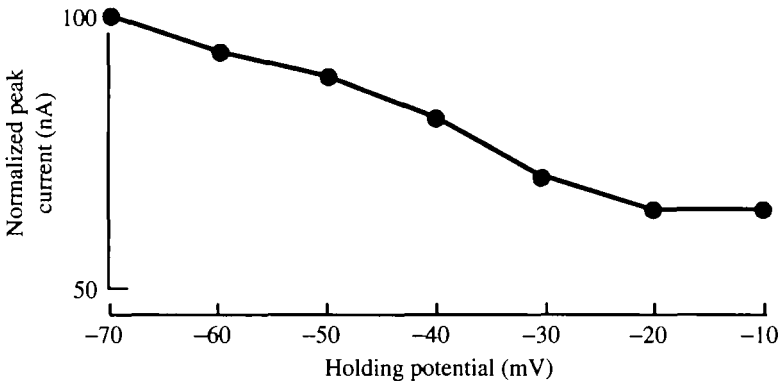


Fig. 5. Effect of holding potential on voltage-activated outward current in a single cell. Leak-subtracted current records; Ca^{2+} -free lanthanum solution; step potential +50 mV. Plot of the peak current amplitude as a percentage of the value obtained with a holding potential of -70 mV against holding potential. As the holding potential was reduced, the peak amplitude of the outward current was observed to decline, indicating that only a component of the outward current (34%) was dependent on the holding potential.

Effect of holding potential on peak K^+ current amplitude

Steady-state inactivation was studied by holding cells at potentials between -70 mV and -10 mV and stepping to a potential of +50 mV. The amplitude of the peak K^+ current was reduced in all cells as the holding potential was made more depolarized. The effect of holding potential on K^+ current is plotted in Fig. 5 for a representative cell: the amplitude of peak K^+ currents at +50 mV obtained from different holding potentials was expressed as a percentage of the peak K^+ current obtained from a holding potential of -70 mV. It can be seen that the reduction in peak K^+ current, because of inactivation, was partial, since the current only declined by 34% when very depolarized holding potentials (-20 mV) were used. Similar results were obtained from three other cells.

The selective effect of inactivation on the early component (the peak) of the K^+ current and the fact that only part of the K^+ currents may be inactivated by very depolarized holding potentials (Figs 4 and 5) suggest that the K^+ currents may be divided into two currents corresponding to an inactivating K^+ current and a non-inactivating K^+ current.

Effect of 4-AP on the outward current

A rapidly inactivating, transient K^+ current, known as I_a , and a slowly inactivating current, known as I_k , are prominent features of many other cells (e.g. Connor and Stevens, 1971; Neher, 1971; Kostyuk *et al.* 1981; Thompson, 1977; Belluzzi *et al.* 1985). The I_a currents of these cells are selectively blocked by the potassium channel antagonist 4-AP.

The effect of 5 mmol l^{-1} 4-AP on the K^+ currents of *Ascaris* was therefore examined using cells bathed in a lanthanum solution and given depolarizing steps to between -25 mV and +55 mV from a holding potential of -35 mV (Fig. 6A). The currents obtained in the presence of 4-AP showed an increase in the time to peak and a decrease in the peak amplitude (Fig. 6B). At a potential of +55 mV the amplitude of the current was

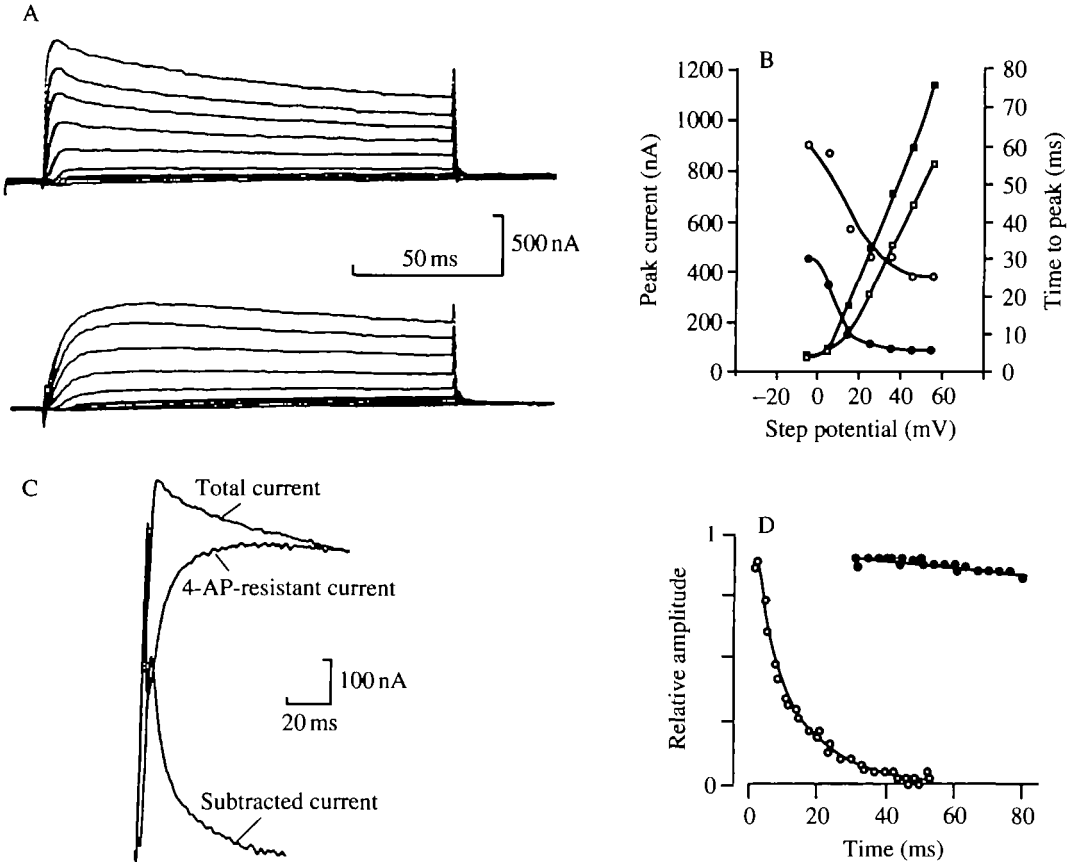


Fig. 6. Effect of 4-AP on leak-subtracted currents. (A) The upper set of currents is from a cell bathed in lanthanum solution and the lower set of currents is from the same cell bathed in 5 mmol l^{-1} 4-AP Ca^{2+} -free lanthanum solution. The holding potential was -35 mV and the cell was stepped to -25 mV , -15 mV , -5 mV , $+5 \text{ mV}$, $+15 \text{ mV}$, $+25 \text{ mV}$, $+35 \text{ mV}$, $+45 \text{ mV}$ and $+55 \text{ mV}$. The currents in 4-AP show the loss of a fast component to the outward current, 37°C . (B) Peak outward current and time to peak plotted against step potential before and after 5 mmol l^{-1} 4-AP. Time to peak before 4-AP, filled circles; after 4-AP, open circles. Peak amplitude before 4-AP, filled squares; after 4-AP, open squares. (C) Current records from a cell obtained with a step potential of $+55 \text{ mV}$ showing the 4-AP-sensitive current obtained by subtracting the 4-AP-resistant current from the control current. Upper trace, control in lanthanum solution; an initial capacitive surge is followed by a rapid rise of the current to a peak of 820 nA in 10 ms . Middle trace, in 5 mmol l^{-1} 4-AP lanthanum solution, shows the 4-AP-resistant current; the current shows a slow rise to a peak of 660 nA after 45 ms and the current decays with a rate constant of 1.1 s (fitted line). Lower trace, 4-AP-sensitive current obtained by subtraction. This current shows a rapid rise to a peak of 425 nA after 10 ms . (D) The decay of the 4-AP-sensitive current (open circles) is rapid with a time constant of 7.53 ms (fitted line) compared to the decay of the 4-AP-resistant current (filled circles; time constant for decay 1.1 s).

reduced to around 70% of its original value; washing the preparation for 30 min did not reverse the effect of 4-AP.

The currents obtained after application of 5 mmol l⁻¹ 4-AP were then subtracted from the control records to determine the 4-AP-sensitive current. Fig. 6C shows the currents at +55 mV. It can be seen that the 4-AP-sensitive current was a transient current which rose to a peak and decayed rapidly.

The rate of decay at +55 mV was described by fitting the 4-AP-sensitive current to the equation:

$$I = A \exp(-t/T), \quad (3)$$

where I is the current at time t , T is the time constant of decay and A is the current at time zero. T was 10.4 ms and A was 410 nA; similar results were obtained in six other cells. These results show that 4-AP was acting to block a fast transient component of the outward current. In order to illustrate the relative speed of inactivation shown by the 4-AP-sensitive current, the 4-AP-resistant current was also fitted by the decay equation (equation 3). It was found that the 4-AP-resistant current decayed with a time constant of 1.1 s in the experiment illustrated in Fig. 6C. Similar results were obtained in eight other experiments. Thus, the 4-AP-sensitive current decayed at a rate two orders of magnitude faster than the 4-AP-resistant current at +55 mV.

Activation curves of 4-AP-sensitive and 4-AP-resistant currents

The peak amplitudes of the 4-AP-sensitive and the 4-AP-resistant currents were plotted against the step potential: all the data from the cell shown in Fig. 6, relating the peaks of the 4-AP-sensitive and 4-AP-resistant currents to voltage, are shown in Fig. 7A. The threshold for both currents was near -15 mV but between -15 mV and +25 mV the 4-AP-sensitive current peak was greater.

The activation characteristics of the two K⁺ currents shown in Fig. 7A were analysed by estimating the conductance, g , at different depolarizations according to the relationship:

$$I = g(V - E_k), \quad (4)$$

where I refers to the peak current values, V is the step potential and E_k is the reversal potential; this equation assumes that the instantaneous current-voltage relationship is linear. The data were then fitted to the Boltzmann equation:

$$g = g_{\max} / \{ 1 + \exp[(V_h - V)/k] \}, \quad (5)$$

where g is the conductance, g_{\max} is the maximum conductance, V is the test potential, V_h is the 'half-activation' potential and k defines the slope. For the 4-AP-sensitive current the peak conductance was 5.3 μ S, V_h was 14.1 mV and k was 10.5 mV; for the 4-AP-resistant current the peak conductance was 9.4 μ S, V_h was 29.3 mV and k was 12.1 mV. The activation curve and the Boltzmann fit to the observations are shown in Fig. 7B: this figure is further evidence of the separate nature of the two K⁺ currents and that the 4-AP-resistant current has a V_h which is 15 mV more positive than that of the 4-AP-sensitive current. The values of 10.5 mV and 12.1 mV for the slope, k , are similar to those obtained in other cells for potassium currents (e.g. squid axon, 12 mV, Hodgkin and Huxley, 1952; rat sympathetic neurone, 10 mV, Belluzzi *et al.* 1985). The values 10.5 mV and 12.1 mV

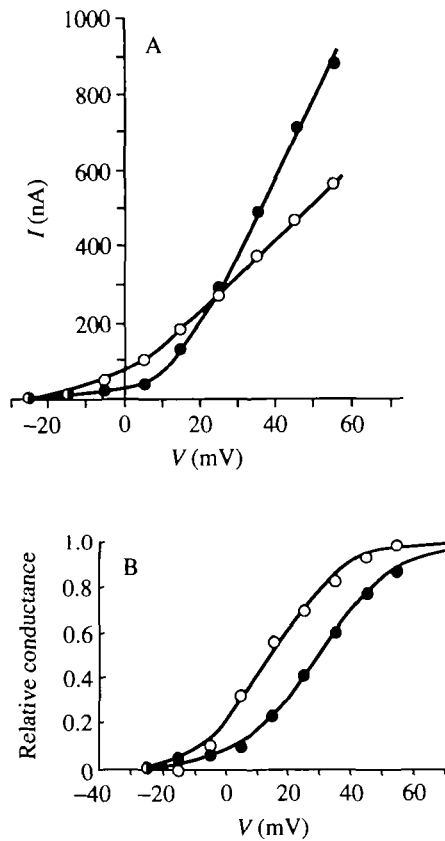


Fig. 7. (A) Peak current–voltage relationship for the 4-AP-sensitive (open circles) and 4-AP-resistant (filled circles) currents. Data from the experiment illustrated in Fig. 6A. (B) Activation curve for the 4-AP-sensitive and 4-AP-resistant currents fitted to Boltzmann equation; see text for further details.

in *Ascaris* for the slopes suggest that the gating charge for opening the 4-AP-sensitive channel is $24/10.5$ (Hille, 1984), i.e. equivalent to 2.3 elementary charges and that for the 4-AP-resistant current is equivalent to 2.0 elementary charges.

Discussion

Our main conclusion is that a voltage-sensitive Ca^{2+} current and two K^{+} currents can be isolated and observed in the soma of muscle cells of *Ascaris suum*. The large amplitude and relatively fast kinetics are consistent with these currents in combination generating the spike potentials described by Weisblat *et al.* (1976). Slower and smaller-amplitude currents which may underlie ‘slow waves’ and ‘modulation waves’ were not revealed in this study. It was pointed out in Materials and methods that low- Ca^{2+} solutions, as used in this study, were likely to abolish currents activated as a result of calcium entry. Thus, Ca^{2+} -activated channel currents could be present and be involved in the production of the slow waves and modulation waves.

Exogenous neural control and initiation of each spike potential at an initiation zone in the syncytium have been suggested for *Ascaris* (DeBell *et al.* 1963); the spikes were suggested to start at the syncytium and then to propagate actively or electrotonically *via* the arm to the rest of the muscle cell. The observations reported here show that the bag region (soma) possesses currents that could initiate spike potentials. It is therefore suggested that each muscle cell of *Ascaris* is capable of self-generated depolarizing activity and that the role of the electrical coupling at the syncytial region is to produce coordination of the depolarization of adjacent muscle cells for contraction of the body wall. The excitatory and inhibitory chemical synaptic inputs at the syncytium could speed or slow the depolarizations.

Ca²⁺ current

Two major types of Ca²⁺ current have been described in other cell types. There is a transient Ca²⁺ current which has been variously named low-threshold inactivating, LTI (see Kostyuk *et al.* 1988), transient (Bossu *et al.* 1985), low-voltage activated, LVA (Carbone and Lux, 1984), T (Fox *et al.* 1987) and type 1 (Narahashi *et al.* 1987). This current is transient and inactivates with a time constant in the region of 20 ms, may be activated at relatively negative potentials (−40 to −20 mV) but also requires relatively negative potentials (more negative than −40 mV) to remove inactivation. The second type of Ca²⁺ current seen in many cells decays slowly with a time constant of at least 1 s. It could be activated from less negative holding potentials than the transient current and has been referred to as high-threshold inactivating, HTI (Kostyuk *et al.* 1988), high-voltage activated HVA (Carbone and Lux, 1984) and L (Fox *et al.* 1987).

The Ca²⁺ current of *Ascaris* seen in our experiments had some but not all of the properties of both of these two major types of Ca²⁺ current: it inactivated but required a relatively depolarized potential for activation and was not inactivated by a holding potential of −35 mV. The current allows the production of a spike in *Ascaris* muscle cells with a resting membrane potential around −35 mV.

Little pharmacology has been done on the Ca²⁺ spikes of *Ascaris* but the report of Wann (1987) shows that the vertebrate Ca²⁺ antagonists verapamil and cinnarazine have little effect in *Ascaris*; the channel may therefore have a distinctive pharmacology.

K⁺ currents

It has already been pointed out in this paper that two major types of K⁺ current have been recognised in a wide variety of cells and that these types are referred to as I_a and I_k. The I_a is a transient current which significantly inactivates with time constants of 10–50 ms at holding potentials more depolarized than −40 mV (Connor and Stevens, 1971; Kostyuk *et al.* 1975; Thompson, 1977) and is usually blocked specifically by 4-AP (Connor and Stevens, 1971; Cook, 1988; but see Yeh *et al.* 1976; Ginsborg *et al.* 1991). The I_k current is a maintained current which is not significantly inactivated at holding potentials more depolarized than −40 mV (Connor and Stevens, 1971; Kostyuk *et al.* 1975; Thompson, 1977).

In this paper the K⁺ current of *Ascaris* was separated into two components on the grounds that maintained depolarization and 4-AP selectively blocked a lower-threshold

($V_h=+14$ mV) transient component (inactivation rate about 10 ms) but left a maintained current (inactivation rate constant about 1 s) which required greater depolarization ($V_h=+29$ mV) to produce activation. The 4-AP-sensitive current of *Ascaris* is therefore I_a -like and the 4-AP-resistant current is I_k -like.

The function of I_a currents as suggested by Connor and Stevens (1971) for neurones of *Anisodoris* is to serve as a damper on the interspike interval to space successive action potentials. This is also possible in *Ascaris* because inactivation of the I_a -like current appears to be complete at -20 mV (Fig. 5B). Activation occurs at potentials more positive than -30 mV (Fig. 7B) so that, at the steady state, only a small fraction of the channels may conduct in the narrow range of -30 mV to -20 mV. At the typical membrane potential of -35 mV, most of the I_a -like current would be inactivated. At the end of a Ca^{2+} spike the subsequent hyperpolarization removes inactivation of the I_a -like channel as well as closing the I_k -like channel and allowing the membrane to depolarize slowly again; the I_a -like current at this stage activates and slows the rate of depolarization until it becomes inactivated; the cell can then again reach threshold. Rates of recovery from inactivation are significant and have to be sufficiently rapid if the I_a -like current is going to behave in this manner. In this study most of the recovery of the transient current took place in less than 1 s but full recovery did not occur until after 12 s. Comparable recovery rates have been seen in *Archidoris* and *Anisodoris* neurones (Aldrich *et al.* 1979) and in the neural somata of *Helix pomatia* (Kostyuk *et al.* 1975; Heyer and Lux, 1976). This slow recovery from inactivation may permit the K^+ currents to contribute to the production of the 'slow waves' and 'modulation waves' of Weisblat *et al.* (1976). This effect and the effect of possible Ca^{2+} -activated channel currents are subjects for further investigation.

We are pleased to acknowledge the financial support of the SERC.

References

- ALDRICH, R. W., GETTING, P. A. AND THOMPSON, S. H. (1979). Inactivation of delayed outward current in molluscan somata *J. Physiol., Lond.* **291**, 507–530.
- BELLUZZI, O., SACCHI, O. AND WANKE, E. (1985). A fast transient outward current in the rat sympathetic neurone studied under voltage-clamp conditions. *J. Physiol., Lond.* **358**, 91–108.
- BOSSU, J. L., FELTZ, A. AND THOMANN, J. M. (1985). Depolarization elicits two distinct calcium currents in vertebrate sensory neurones. *Pflügers Arch.* **403**, 360–368.
- BRADING, A. F. AND CALDWELL, P. C. (1971). The resting membrane potential of the somatic muscle cells of *Ascaris lumbricoides*. *J. Physiol., Lond.* **217**, 605–624.
- CARBONE, E. AND LUX, H. D. (1984). A low voltage-activated, fully inactivating Ca channel in vertebrate sensory neurones. *Nature* **310**, 501–502.
- CONNOR, J. A. AND STEVENS, C. F. (1971). Voltage-clamp studies of a transient outward membrane current in gastropod neural somata. *J. Physiol., Lond.* **213**, 21–30.
- COOK, N. S. (1988). The pharmacology of potassium channels and their therapeutic potential. *Trends pharmac. Sci.* **9**, 21–28.
- DEBELL, J. T., DEL CASTILLO, J. AND SANCHEZ, V. (1963). Electrophysiological of somatic muscle cells of *Ascaris lumbricoides*. *J. cell. comp. Physiol.* **62**, 159–177.
- FENWICK, E. M., MARTY, A. AND NEHER, E. (1982). Sodium and calcium channels of bovine chromaffin cells. *J. Physiol. Lond.* **331**, 599–636.
- FOX, A. P., NOWYCKY, M. C. AND TSIEN, R. W. (1987). Kinetic and pharmacological properties

- distinguishing three types of calcium channel in chick sensory neurones. *J. Physiol., Lond.* **394**, 173–200.
- GINSBORG, B. L., MARTIN, R. J. AND PATMORE, L. (1991). On the sodium and potassium currents of a human neuroblastoma cell line. *J. Physiol., Lond.* **434**, 121–149.
- HEYER, C. B. AND LUX, H. D. (1976). Control of the delayed outward potassium currents in bursting pacemaker neurones of the snail, *Helix pomatia*. *J. Physiol., Lond.* **262**, 349–382.
- HILLE, B. (1984). *Ionic Channels of Excitable Membranes*. Sunderland, MA: Sinauer.
- HODGKIN, A. L. AND HUXLEY, A. F. (1952). A quantitative description of membrane current and its application to conduction and excitation in nerve. *J. Physiol., Lond.* **117**, 500–544.
- JARMAN, M. AND ELLORY, J. C. (1969). Effect of TTX on *Ascaris* somatic muscle. *Experientia* **25**, 507.
- KOSTYUK, P. G., KRISHTAL, O. A. AND DOROSHENKO, P. A. (1975). Outward currents in isolated snail neurones. I. Inactivation kinetics. *Comp. Biochem. Physiol.* **51C**, 259–263.
- KOSTYUK, P. G., SHUBA, YA. M. AND SAVCHENKO, A. N. (1988). Three types of calcium channels in mouse sensory neurones. *Pflügers Arch.* **411**, 661–669.
- KOSTYUK, P. G., VESELOVSKY, N. S., FEDULOVA, S. A. AND TSYNDRENKO, A. Y. (1981). Ionic currents in the somatic membrane of rat dorsal root ganglion neurones. III. Potassium currents. *Neuroscience* **6**, 2439–2445.
- LEE, K. S. AND TSIEN, R. W. (1982). Reversal of current through calcium channels in dialysed single heart cells. *Nature* **297**, 498–501.
- MARTIN, R. J. (1982). Electrophysiological effects of piperazine and diethylcarbamazine on *Ascaris suum* somatic muscle. *Br. J. Pharmac.* **77**, 255–265.
- MEECH, R. W. AND STANDEN, N. B. (1975). Potassium-activation in *Helix aspera* neurones under voltage clamp: a component mediated by calcium influx. *J. Physiol., Lond.* **249**, 211–240.
- NARAHASHI, T., TSUNOO, A. AND YOSHI, M. (1987). Characterization of two types of calcium channels in mouse neuroblastoma cells. *J. Physiol., Lond.* **383**, 231–249.
- NEHER, E. (1971). Two fast transient current components during voltage clamp on snail neurones. *J. gen. Physiol.* **58**, 36–53.
- REUTER, H. AND SCHOLTZ, H. (1977). A study of the ion selectivity and kinetic properties of the calcium dependent slow inward current in mammalian cardiac muscle. *J. Physiol., Lond.* **264**, 17–47.
- ROSENBLUTH, J. (1963). Fine structure of body muscle cells and neuromuscular junctions in *Ascaris lumbricoides*. *J. Cell Biol.* **19**, 82A.
- ROSENBLUTH, J. (1965). Ultrastructure of somatic muscle cells in *Ascaris lumbricoides*. II. Intermuscular junctions, neuromuscular junctions and glycogen stores. *J. Cell Biol.* **26**, 579–591.
- THOMAS, M. V. (1984). Voltage-clamp analysis of a calcium-mediated potassium conductance in cockroach (*Periplaneta americana*) central neurones. *J. Physiol., Lond.* **350**, 159–178.
- THOMPSON, S. H. (1977). Three pharmacologically distinct potassium channels in moluscan neurones. *J. Physiol., Lond.* **265**, 465–488.
- THORN, P. AND MARTIN, R. J. (1987). A high-conductance Ca-dependent chloride channel in *Ascaris suum* muscle. *Q. Jl exp. Physiol.* **72**, 31–49.
- WANN, K. T. (1987). The electrophysiology of the somatic muscle cells of *Ascaris lumbricoides* and *Ascaridia galli*. *Parasitology* **94**, 555–566.
- WEISBLAT, D. A., BYERLY, L. AND RUSSELL, R. L. (1976). Ionic mechanisms of electrical activity in somatic muscle of the nematode *Ascaris lumbricoides*. *J. comp. Physiol. A* **111**, 93–113.
- YEH, J. Z., OXFORD, G. S., WU, C. H. AND NARAHASHI, T. (1976). Dynamics of aminopyridine block of potassium channels in squid axon membrane. *J. gen. Physiol.* **68**, 519–535.